Mechanistic Investigations on the Belousov−Zhabotinsky Reaction with Oxalic Acid Substrate. 2. Measuring and Modeling the Oxalic Acid−Bromine Chain Reaction and Simulating the Complete Oscillatory System

Krisztina Pelle, Maria Wittmann,* Klára Lovrics, and Zoltán Noszticzius

Center for Complex and Nonlinear Systems and the Department of Chemical Physics, Budapest University of Technology and Economics, H-1521 Budapest, Hungary

Received: June 11, 2004; In Final Form: July 12, 2004

The aim of the present paper is to study radical reactions important in the mechanism of the Belousov−Zhabotinsky (BZ) reaction with its simplest organic substrate, oxalic acid, and to model the oscillatory system applying the newly determined rate constants. We considered five radical species in this BZ system: carboxyl radical, bromine atom, dibromine radical ion, and bromine monoxide and dioxide radicals. To study separately reactions of only three radicals, $^{\bullet}CO_2H$, $^{\bullet}Br$, and $^{\bullet}Br_2^-$, semibatch experiments were performed. The semibatch reactor contained oxalic acid, elemental bromine, and bromide ions in a solution of 1 M H_2SO_4 at 20 °C, and a continuous inflow of Ce^{4+} generated carboxyl radicals. The carboxyl radicals initiate a chain reaction: first they react with elemental bromine and produce bromine atoms (CR1); then the bromine atoms react with oxalic acid, producing carboxyl radicals again (CR2). Consumption of elemental bromine in the chain reaction was followed with a bright Pt electrode. By measuring the stoichiometry of the chain reaction, it was possible to determine or estimate several rate constants. It was found that CR1 is a fast reaction with an estimated k value of more than 10^9 M^{-1} s^{-1}. The rate constant of CR2 is 7×10^5 M^{-1} s^{-1}, and the k value for the $Ce^{4+}-{}^{\bullet}CO_2H$ reaction is 1.5×10^9. These values were obtained by comparing experiments with model calculations. Such simulations also suggested that a reaction of $^{\bullet}Br_2^-$ with oxalic acid, analogous to CR2, plays a negligible role or no role here. Simulations of the oscillatory system applied rate constants, which were known from the literature, or determined here or in the first part of our work, and some unknown rate constants were estimated on the basis of analogous radical reactions. To obtain an optimal fit between experiments and simulations, only one rate constant was used as a variable parameter. This was the reaction of carboxyl radical with acidic bromate with an optimal k value of 1.0×10^7 M^{-1} s^{-1}. Agreement between experimental and simulated oscillations was satisfactory at low bromine removal rates (that rate was controlled by a nitrogen gas flow), but a disagreement was found at higher flow rates. Possible reasons for this disagreement are discussed in the conclusion.

1. Introduction

This is the second part of our investigations on the mechanism of the Belousov−Zhabotinsky (BZ) reaction with oxalic acid substrate. As was pointed out in the first part,[1] oxalic acid is the simplest organic substrate of the BZ reaction and also an important intermediate[2] in the classical BZ reaction,[3,4] where the substrate is malonic acid. When oxalic acid is the only substrate, however, oscillatory dynamics requires a continuous removal of the end product bromine in 1 M sulfuric acid medium.[5] The measured "rate constant" of the physical removal of bromine by an inert gas flow together with the experimentally observed oscillations in the CO_2 production were reported in the first part. In that previous work we also determined the rate constants of the oxygen atom transfer reactions from three molecular oxybromine species (hypobromous and bromous acids and acidic bromate) to the oxalic acid substrate. Those nonradical processes can occur even in the absence of the cerium catalyst. Nevertheless, if cerium ions are introduced into the acidic bromate−oxalic acid system, then radical processes appear as well. Studying these radical reactions, and modeling the complete oscillating system, are the aim of the present paper.

Radical processes start with the oxidation of Ce^{3+} to Ce^{4+}, the mechanism of that step is well-known,[2,4,6] however. The next step is the Ce^{4+}−oxalic acid reaction

$$Ce^{4+} + (COOH)_2 \rightarrow CO_2 + H^+ + Ce^{3+} + {}^{\bullet}CO_2H \qquad \text{(CR0)}$$

which was also studied by various authors.[2,7] What is not yet studied experimentally, however, is the further reactions of the very reactive carboxyl radical produced in (CR0). In the BZ system with oxalic acid substrate, most of the further radical processes are initiated by that primary carboxyl radical. The carboxyl radical is a protonated form of the well-documented carbon dioxide radical anion.[8] As the pK_a value[9] for $^{\bullet}CO_2H$ is 1.4, in our acidic medium ($[H^+] = 1.29$ M) the radical occurs mostly in its protonated form ($[^{\bullet}CO_2^-]/[^{\bullet}CO_2H] \approx 0.03$). It is assumed that protonation causes only minor changes in kinetics, although this has not been studied in detail.[8] Experimental data, however, are available mostly for the reactions of the carbon dioxide radical ion,[8] and these data will be applied here as well, neglecting this way any difference due to the protonation of the radical. The $^{\bullet}CO_2^-$ radical is a strongly reducing species with a redox potential of −2.0 V vs NHE.[9] It transfers an electron very rapidly to various organic and inorganic compounds.[8]

* Corresponding author. E-mail: wittmann@eik.bme.hu.

10.1021/jp047472a CCC: $27.50
Published on Web 08/24/2004

The $^{\bullet}CO_2H$ radical produced in (CR0) can react with several reactants and intermediates of a BZ oscillator. The reaction partners are Ce^{4+}, all the oxybromine species, and elementary bromine. Among the reactions of the carboxyl radical with various bromine species, we were able to study only one process separately from the others: the process that starts with the carboxyl radical−elementary bromine reaction. That process was found to be a radical chain reaction with the following steps of chain propagation:

$$^{\bullet}CO_2H + Br_2 \rightarrow CO_2 + H^+ + Br^- + {}^{\bullet}Br \qquad \text{(CR1)}$$

$$^{\bullet}Br + (COOH)_2 \rightarrow CO_2 + H^+ + Br^- + {}^{\bullet}CO_2H \qquad \text{(CR2)}$$

followed by radical−radical type chain termination reactions, or chain termination by the Ce^{4+}−carboxyl radical reaction. While CR1, and also the chain termination reactions, are fast reactions with rate constants close to the diffusion controlled values, CR2 should be much slower. Consequently, it seemed reasonable that k_{CR2} could be measured with some experiments, where the observed stoichiometry could provide data about the average chain length. It was also realized that a semibatch reactor could be applied advantageously in the planned experiments, which need a constant source of carboxyl radicals. Thus designing and performing such experiments to collect evidence for CR1, and to measure k_{CR2}, were among the main objectives of the research presented here.

The final aim is, however, to perform model calculations for the full oscillating system with all the available and the newly collected rate constants, and to compare the results with the experimentally observed oscillations reported previously.[1] To this end we collected the rate constants of other radical reactions, which were not determined here, but were reviewed in the literature.[8] If data for a certain rate constant were missing, then a value for an analogous reaction was regarded as a basis of estimate.

2. Experimental Section

2.1. Chemicals. Oxalic acid (Reanal p.a.), $Ce(SO_4)_2 \cdot 4H_2O$ (Merck, p.a.), $NaBrO_3$ (Fluka, puriss), NaBr (Merck, p.a.), and H_2SO_4 97% (J. T. Baker) were used as received. All solutions were prepared with doubly distilled water. Stock solutions containing bromine and bromide, and also the reaction mixture for the semibatch reactor, were prepared freshly.

2.2. Semibatch Experiments To Study the Oxalic Acid−Bromine Chain Reaction. The experiments were performed in a magnetically stirred 60 mL beaker (it contained 48 mL liquid at the start and about 48.5 mL at the end of an experiment) surrounded by a thermostated jacket (temp. 20 °C). A light shield was applied to prevent any light-induced reaction from occurring in the reactor. The reactor was operated in a semibatch configuration with a continuous Ce^{4+} inflow (input concentrations: $[Ce^{4+}] = 0.2$ M, $[H_2SO_4] = 1$ M) provided by a controllable peristaltic pump (input flow rates measured in μL/min: 12, 24, 48, and 96). We applied a tubing in the peristaltic pump with the smallest available inner diameter (0.18 mm) leading directly to the reactor to maintain a relatively high linear velocity inside the tubing (~8 mm/s) even at the lowest input flow rate. The bromine concentration in the reactor was monitored with a platinum indicator electrode. The reference electrode was Ag/AgCl submerged into a solution containing both KCl and H_2SO_4 in 1 M concentration. The reference electrode was connected to the reactor via a salt bridge filled with 1 M H_2SO_4. (The presence of the sulfuric acid both in the reference solution and in the salt bridge helped to keep the otherwise somewhat unstable liquid−liquid junction potentials at a low value. The absolute potential was not important in this experiment.)

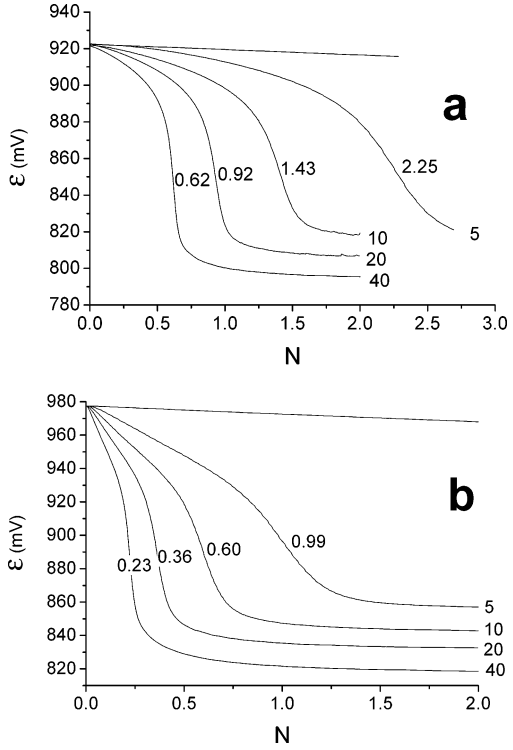

Figure 1. Reduction of bromine by carboxyl radicals generated in the Ce^{4+}−oxalic acid reaction. Measured platinum electrode potential vs the stoichiometric ratio $N = n(Ce^{4+})_t/n(Br_2)_0$ diagrams for various Ce^{4+} input rates. (See the Experimental Section for the applied notation.) N_{EP} (the value of N at the inflection point) is indicated on the curves. Ce^{4+} inflow rate: 2×10^{-3} M/$\Delta\tau$, where $\Delta\tau$ is the time necessary to raise the stoichiometric ratio to 2. Individual $\Delta\tau$ parameter values (5, 10, 20, and 40 min) are indicated at the end of each curve. The "reference batch" curve is an electrode potential vs time diagram in the absence of any Ce^{4+} input. See text for further explanations. Initial concentrations: $[Br_2]_0 = 10^{-3}$ M, $[OA]_0 = 0.2$ M, $[H_2SO_4] = 1$ M, (a) (high bromide) $[Br^-]_0 = 10^{-2}$ M, (b) (low bromide) $[Br^-]_0 = 10^{-3}$ M.

The experiment was started with the following initial concentrations: [OA] = 0.2 M, $[Br_2]$ = 1 mM, $[Br^-]$ = 10 mM (or 1 mM in a second series of experiments), and $[H_2SO_4]$ = 1 M in a total volume of 48 mL. These initial conditions were established by mixing 19.2 mL of 0.5 M oxalic acid solution (in water) with 16.8 mL of water, 4 mL of 10 M H_2SO_4, and 8 mL of bromine−bromide solution: 60 mM (or 6 mM) Br^- and 6 mM Br_2 in 1 M sulfuric acid.

In each experiment 0.48 mL of the Ce^{4+} solution was pumped into the semibatch reactor, thus the total reaction time was 5, 10, 20, or 40 min depending on the input flow rate. Carboxyl radicals that were generated in the Ce^{4+}−oxalic acid reaction gradually reduced the bromine content of the reactor to bromide. The decrease of the bromine concentration was indicated by a falling Pt electrode potential, which followed a titration type curve. An inflection point in the potential vs time diagram indicated the equivalence point, where the initial bromine was reduced to bromide. To determine the experimental chain length, these potential−time diagrams were transformed to potential vs stoichiometric ratio $N = n(Ce^{4+})_t/n(Br_2)_0$ diagrams, as it shown in Figure 1. Here $n(Ce^{4+})_t$ is the amount (in moles) of the Ce^{4+} pumped into the reactor since the start of the experiment and $n(Br_2)_0$ is the amount of bromine present initially in the reactor. Thus the abscissa for most of the curves is not

the time, but the above-mentioned stoichiometric ratio. The only exception is the "batch experiment" curve, which is an electrode potential vs time diagram. That experiment was carried out without a Ce^{4+} inflow, to measure the bromine loss not related to the chain reaction. It illustrates that, without a Ce^{4+} inflow, platinum potential changes are negligible in the time span of the experiments.

3. Results and Discussion

Before modeling the complete system, it is desirable to study as many processes separately as possible. That can be a difficult task especially in the case when the intermediates are free radicals. Fortunately, it was possible to find a subsystem where the reactions of only three radicals could be studied separately. This is the oxalic acid−bromine chain reaction.

3.1. Observation of a Radical Chain Mechanism in the Oxalic Acid−Bromine Reaction. As discussed in the Introduction, the chain reaction is initiated and maintained by the carboxyl radicals, produced in the Ce^{4+}−oxalic acid reaction (CR0). The experiments were performed by pumping Ce^{4+} solution into a semibatch reactor containing oxalic acid, elementary bromine, and bromide in 1 M sulfuric acid, as described in the Experimental Section.

3.2. Batch Experiments with No Ce^{4+} Inflow. It is important that in the absence of Ce^{4+} inflow the molecular reaction between bromine and oxalic acid be slow. That can be achieved by establishing an initial bromide level in the reactor. This is because in the molecular mechanism[10] of that reaction the active intermediate is the hypobromous acid produced in the hydrolysis of bromine, and the hydrolysis is suppressed in the presence of bromide ions. Thus in the case of batch experiments a very slow bromine consumption can be observed, which is due partly to the HOBr−oxalic acid reaction, and partly to some evaporation losses of bromine. To separate these two effects, we made blank experiments without oxalic acid.

When no oxalic acid was present (other concentrations were the same as in the real experiments: $[H_2SO_4] = 1$ M, $[Br_2] = 1$ mM, $[Br^-] = 1$ or 10 mM), the observed potential drop was due exclusively to the evaporation of bromine from the stirred solution. The evaporation rate is proportional to the bromine concentration, and the "rate constant" k_{EV} of this process can be calculated from the rate of the observed electrode potential decrease $d\epsilon/dt$, as given in Appendix A. According to our measurements $d\epsilon/dt = -(3.1 \pm 0.3) \times 10^{-3}$ mV/s, thus $k_{EV} = (2.5 \pm 0.25) \times 10^{-4}$ s^{-1}. This result was independent of the bromide concentration between 1 and 10 mM. (The deviations found between the parallel experiments are due to some uncontrolled changes in the hydrodynamic conditions, like the relative position of the Pt electrode, the salt bridge and the magnetic stirrer, which could vary somewhat from one experiment to the other. These experimental conditions could affect the escape of bromine from the stirred liquid to the laboratory atmosphere. These small uncertainties, however, have little or no effect on our results, as the actual value of k_{EV} does not influence the measurements significantly, where other bromine consuming processes dominate.)

In the "batch" experiment oxalic acid was already present ($[(COOH)_2] = 0.2$ M, other concentrations as before); thus in this case the decrease of the bromine concentration was due to a combination of two effects: (i) the physical escape of bromine from the solution as discussed above and (ii) the chemical reaction of bromine with oxalic acid.

Now we are interested in the latter. Again, the rate of the Pt potential drop was measured, which was $d\epsilon/dt = -3.4 \times 10^{-3}$ mV/s with $[Br^-]_0 = 1$ mM, and $d\epsilon/dt = -3.1 \times 10^{-3}$ mV/s with $[Br^-]_0 = 10$ mM. As can be seen from the $d\epsilon/dt$ values, even in the case of the experiment with 1 mM bromide, still the physical escape of bromine was dominant, and the contribution of the chemical reaction was only just above the experimental error.[11]

It is important to remark that a significant chain reaction can be initiated without a light shield, even by the scattered light from the lamps in the laboratory, if both bromine and oxalic acid are present. For example, in the case of the batch experiment with 1 mM bromide, the measured slope $d\epsilon/dt$ can be increased by 1 order of magnitude, simply by removing the light shield, even without any direct illumination of the reactor.

3.3. Results of the Semibatch Experiments with Different Flow Rates: Stoichiometries Supporting the Chain Mechanism of the Reaction. The immediate aim of the semibatch experiments was to prove experimentally that the carboxyl radicals, generated in the Ce^{4+}−oxalic acid reaction, are able to reduce elemental bromine to bromide in a fast reaction. This was expected because the carboxyl radical (like carbon dioxide radical ion) is a very strong reducing agent; moreover, an analogous reaction between elemental iodine and carbon dioxide radical ions was already known[8]

$$^{\bullet}CO_2^- + I_2 \rightarrow CO_2 + {}^{\bullet}I_2^-$$

with a rate constant of 7×10^9 M^{-1} s^{-1}. $^{\bullet}Br_2^-$ radical ions produced in the analogous process

$$^{\bullet}CO_2H + Br_2 \rightarrow CO_2 + {}^{\bullet}Br_2^- + H^+ \qquad \text{(R33)}$$

can recombine in reaction R21 (see Table 1) or can be reduced further to bromide by the next carboxyl radical, in a fast radical−radical reaction:

$$^{\bullet}Br_2^- + {}^{\bullet}CO_2H \rightarrow CO_2 + 2Br^- + H^+ \qquad \text{(R37)}$$

(Here the numbering of the reactions is the same as in Table 1.) As one Ce^{4+} generates one carboxyl radical, we expected a stoichiometry where the reduction of one bromine molecule requires at least two Ce^{4+} ions. (That is $N_{EP} = n(Ce^{4+})_{EP}/n(Br_2)_0 \geq 2$, where N_{EP} is the stoichiometric number in the equivalence point. We expected that more than two Ce^{4+} ions would be required, regarding the Ce^{4+} loss due to the side reaction R34, the reduction of Ce^{4+} by carboxyl radicals, and also a carboxyl radical loss due to R38, the disproportionation of those radicals.)

Already the first preliminary experiments showed that carboxyl radicals are really able to reduce bromine to bromide, as we obtained characteristic "titration curves" (see Figure 1) with an inflection point indicating when the bromine was consumed. The measured stoichiometric number N_{EP}, however, was not larger, but smaller than 2. That observation suggested that we found a chain reaction where free $^{\bullet}Br$ atoms, which are in a fast equilibrium with dibromine radical ions, or $^{\bullet}Br_2^-$ radical ions themselves, attack the oxalic acid molecules in reaction R29 or in R40, to produce further carboxyl radicals. Such a reaction between bromine atoms and oxalic acid was assumed already by Field and Boyd[12] and by Hlaváčová and Ševčik,[13] but without direct experimental evidence.

In the next step, to prove the chain reaction hypothesis, we carried out semibatch experiments with different flow rates. In the case of a chain reaction, lowering the flow rates ought to decrease N_{EP}, as the chain length should be longer in that case. The explanation for that is the following. At lower flow rates the steady-state concentration of Ce^{4+}, and therefore that of the

TABLE 1: Reactions and Rate Constants of the Cerium-Catalyzed BZ Reaction with Oxalic Acid Substrate

no.	reaction			rate constants: forward		rate constants: reverse		ref
RG	Br_2 (dissolved)	→	Br_2 (in the gas phase)	variable	s^{-1}	0		1
R1	$Br^- + HOBr + H^+$	→	$Br_2 + H_2O$	8×10^9	$M^{-2}\,s^{-1}$	110	s^{-1}	2
R2	$Br^- + HBrO_2 + H^+$	→	2HOBr	2.9×10^6	$M^{-2}\,s^{-1}$	2.0×10^{-5}	$M^{-1}\,s^{-1}$	2
R3	$Br^- + BrO_3^- + 2H^+$	→	$HOBr + HBrO_2$	f(conc)[b]	$M^{-3}\,s^{-1}$	3.2	$M^{-1}\,s^{-1}$	2
R4	$HBrO_2 + H^+$	→	$H_2BrO_2^+$	2×10^6	$M^{-1}\,s^{-1}$	1.0×10^8	s^{-1}	2
R5	$HBrO_2 + H_2BrO_2^+$	→	$HOBr + BrO_3^- + 2H^+$	1.7×10^5	$M^{-1}\,s^{-1}$	0		2
R6	$HBrO_2 + BrO_3^- + H^+$	→	$Br_2O_4 + H_2O$	48	$M^{-2}\,s^{-1}$	3.2×10^3	s^{-1}	2
R7	Br_2O_4	→	$2^\bullet BrO_2$	7.5×10^4	s^{-1}	1.4×10^9	$M^{-1}\,s^{-1}$	2
R8	$Ce^{3+} + {}^\bullet BrO_2 + H^+$	→	$Ce^{4+} + HBrO_2$	6.0×10^4	$M^{-2}\,s^{-1}$	1.3×10^4	$M^{-1}\,s^{-1}$	2
R9	$Ce^{3+} + {}^\bullet BrO + H^+$	→	$Ce^{4+} + HOBr$	10^5	$M^{-2}\,s^{-1}$	0		this work
R10	$Ce^{3+} + Br^\bullet$	→	$Ce^{4+} + Br^-$	1×10^6	$M^{-1}\,s^{-1}$	0		Th, 16
R11	$2BrO_3^- + 2H^+$	→	$2HBrO_2 + O_2$	6.0×10^{-10}	$M^{-3}\,s^{-1}$	0		2
R12	$Br_2 + Br^-$	→	Br_3^-	1×10^8	$M^{-1}\,s^{-1}$	7.5×10^6	s^{-1}	12
R13	$2Br^\bullet$	→	Br_2	3×10^9	$M^{-1}\,s^{-1}$	0		Th
R14	$Br^\bullet + BrO_2^\bullet + H_2O$	→	$HOBr + HBrO_2$	3×10^9	$M^{-1}\,s^{-1}$	0		Th
R15	$Br^\bullet + HOBr$	→	$BrO^\bullet + Br^- + H^+$	4.1×10^9	$M^{-1}\,s^{-1}$	0		8
R16	$Br^\bullet + BrO^\bullet + H_2O$	→	2HOBr	3×10^9	$M^{-1}\,s^{-1}$	0		Th
R17	$Br^\bullet + HBrO_2$	→	$BrO_2^\bullet + Br^- + H^+$	1×10^9	$M^{-1}\,s^{-1}$	0		Th
R18	$Br^\bullet + Br^-$	→	${}^\bullet Br_2^-$	9×10^9	$M^{-1}\,s^{-1}$	5×10^4	s^{-1}	7, 17
R19	${}^\bullet Br_2^- + Br^\bullet$	→	Br_3^-	1.37×10^9	$M^{-1}\,s^{-1}$	0		7, 18
R20	${}^\bullet Br_2^- + Ce^{3+}$	→	$2Br^- + Ce^{4+}$	1×10^3	$M^{-1}\,s^{-1}$	0		Th
R21	$2^\bullet Br_2^-$	→	$Br_3^- + Br^-$	2.2×10^9	$M^{-1}\,s^{-1}$	0		7, 19
R22	$2BrO^\bullet + H_2O$	→	$HOBr + HBrO_2$	2.8×10^9	$M^{-1}\,s^{-1}$	0		20
R23	$OA + HBrO_3$	→	$2CO_2 + HBrO_2$	7.47×10^{-4}	$M^{-1}\,s^{-1}$	0		1
R24	$OA + HBrO_2$	→	$2CO_2 + HOBr$	4.2	$M^{-1}\,s^{-1}$	0		1
R25.1	$OA + HOBr$	→	$2CO_2 + Br^- + H^+$	17	$M^{-1}\,s^{-1}$	0		1
R25.2	$OA + 2HOBr$	→	$2CO_2 + Br_2 + H_2O$	1.2×10^5	$M^{-2}\,s^{-1}$	0		1
R26	$OA + Ce^{4+}$	→	$CO_2 + {}^\bullet COOH + Ce^{3+} + H^+$	f(conc)[c]	$M^{-1}\,s^{-1}$	0		7
R27	$OA + BrO_2^\bullet$	→	$CO_2 + {}^\bullet COOH + HBrO_2$	0 (max. 10)	$M^{-1}\,s^{-1}$	0		1
R28	$OA + BrO^\bullet$	→	$CO_2 + {}^\bullet COOH + HOBr$	100	$M^{-1}\,s^{-1}$	0		Th
R29	$OA + Br^\bullet$	→	$CO_2 + {}^\bullet COOH + Br^- + H^+$	7×10^5	$M^{-1}\,s^{-1}$	0		chain
R30	${}^\bullet COOH + BrO_3^- + H^+$	→	$CO_2 + BrO_2^\bullet$	1.0×10^7	$M^{-2}\,s^{-1}$	0		osc est
R31	${}^\bullet COOH + HBrO_2$	→	$CO_2 + BrO^\bullet$	1×10^8	$M^{-1}\,s^{-1}$	0		Th
R32	${}^\bullet COOH + HOBr$	→	$CO_2 + Br^\bullet$	5.7×10^8	$M^{-1}\,s^{-1}$	0		Th
R33.1	${}^\bullet COOH + Br_2$	→	$CO_2 + {}^\bullet Br_2^- + H^+$	7×10^9	$M^{-1}\,s^{-1}$	0		Th
R33.2	${}^\bullet COOH + Br_3^-$	→	$CO_2 + {}^\bullet Br_2^- + Br^- + H^+$	7×10^9	$M^{-1}\,s^{-1}$	0		Th
R34	${}^\bullet COOH + Ce^{4+}$	→	$CO_2 + Ce^{3+} + H^+$	1.5×10^9	$M^{-1}\,s^{-1}$	0		chain
R35	${}^\bullet COOH + BrO_2^\bullet$	→	$CO_2 + HBrO_2$	5×10^9	$M^{-1}\,s^{-1}$	0		2, 15
R36	${}^\bullet COOH + Br^\bullet$	→	$CO_2 + Br^- + H^+$	8×10^9	$M^{-1}\,s^{-1}$	0		Th
R37	${}^\bullet COOH + {}^\bullet Br_2^-$	→	$CO_2 + 2Br^- + H^+$	7×10^9	$M^{-1}\,s^{-1}$	0		Th
R38	${}^\bullet COOH + BrO^\bullet$	→	$CO_2 + HOBr$	7×10^9	$M^{-1}\,s^{-1}$	0		Th
R39	$2^\bullet COOH$	→	$CO_2 + HCOOH$	5×10^8	$M^{-1}\,s^{-1}$	0		21
R40	$(COOH)_2 + {}^\bullet Br_2^-$	→	$CO_2 + {}^\bullet COOH + 2Br^- + H^+$	0	$M^{-1}\,s^{-1}$	0		chain
R41	$BrO^\bullet + HBrO_2$	→	$HOBr + BrO_2^\bullet$	4×10^8	$M^{-1}\,s^{-1}$	0		22
R42	$BrO^\bullet + BrO_2^\bullet$	→	$2HBrO_2$	1×10^9	$M^{-1}\,s^{-1}$	0		Th, osc est
R43	${}^\bullet Br_2^- + BrO_2^\bullet$	→	$Br_2 + HBrO_2$	3×10^9	$M^{-1}\,s^{-1}$	0		Th
R44	${}^\bullet Br_2^- + BrO^\bullet$	→	$Br_2 + HOBr$	3×10^9	$M^{-1}\,s^{-1}$	0		Th

[a] Abbreviations: ${}^\bullet COOH$ = carboxyl radical, OA = oxalic acid. Th: theoretical estimate based on literature data. Chain: estimate based on chain reaction experiments and simulations. Osc est: estimate from oscillatory experiments and simulations. [b] k_3 can be described by a power series: $k_3 = c_0 + c_1[Br^-/M] + c_2[Br^-/M]^2 + c_3[Br^-/M]^3$ for $[Br^-] > 2 \times 10^{-6}$ M; $k_3 = 0.3$ for $[Br^-] < 2 \times 10^{-6}$ M. $c_0 = 0.48789\ M^{-1}\,s^{-1}$, $c_1 = 0.143911 \times 10^5\ M^{-1}\,s^{-1}$, $c_2 = -0.7076958 \times 10^8\ M^{-1}\,s^{-1}$, and $c_3 = 0.116310 \times 10^{12}\ M^{-1}\,s^{-1}$. In the range of bromide concentrations typical for the BZ system (2×10^{-6} to 2×10^{-5} M), k_3 can be approximated by the mean value $k_3 = 0.6\ M^{-1}\,s^{-1}$. [c] k_{26} can be described by the following power series: $k_{26} = c_0/(1 + c_1[OA] + c_1c_2[OA]^2)$, where $c_0 = 28\ M^{-1}\,s^{-1}$, $c_1 = 135\ M^{-1}$, and $c_2 = 66\ M^{-1}$.

carboxyl radical, bromine atom, and dibromine radical ion would be smaller. As the rates of the chain terminating reactions are proportional with the product of the concentrations of the aforementioned reactive intermediates, the chain terminating rates would decrease with the decreasing flow rates in a nonlinear way, and more rapidly than the rate of the chain propagating reactions. This is because the chain propagating reactions are reactions between molecules and radicals, consequently their rate depends linearly on the radical concentrations. So at lower flow rates, the probability of the chain propagating reactions should increase compared to the chain terminating reactions, and the chain length should also increase as a consequence. The experimental results, obtained with different flow rates as shown in Figure 1a, justifies these expectations: at smaller flow rates the stoichiometric number N_{EP} was also smaller, proving that less chain initiating Ce^{4+} was needed to achieve the quantitative reduction of the initial bromine amount. Thus the results supported the chain reaction hypothesis.

3.4. Estimation of the Kinetic Chain Length ν from an Experiment. The molar amount of bromide ions generated by $n(Ce^{4+})$ is

$$n(Br^-) = (1 + 2\nu)n(Ce^{4+})$$

where ν is the kinetic chain length. This is because from one Ce^{4+} initially one carboxyl radical is formed, which initiates the chain reaction, when it reacts with bromine. (We assume here that carboxyl radicals react exclusively with bromine. This

is a good approximation, as long as enough bromine is present in the reaction mixture.) Thus the chain initiation step produces one bromide ion, and each cycle of the chain propagation adds 2 more, resulting in $1 + 2\nu$ bromide ion after ν cycles. In the equivalence point, the molar amount of bromide ions generated from the start of the experiment is just twice as much as the molar amount of bromine present initially in the reactor:

$$n(Br^-)_{EP} = (1 + 2\nu)n(Ce^{4+})_{EP} = 2n(Br_2)_0$$

From the above relationship the kinetic chain length can be expressed as a function of the stoichiometric number N_{EP}:

$$\nu = 1/N_{EP} - 0.5$$

Thus the chain length of an experiment can be estimated from the stoichiometry of the chain reaction. For example, in Figure 1a ($[Br^-]_0 = 0.01$ M) for $\Delta\tau = 20$ min $N_{EP} = 0.92$; thus the kinetic chain length $\nu = 0.59$. In the same figure for $\Delta\tau = 40$ min $N_{EP} = 0.62$ so $\nu = 1.11$. The largest kinetic chain length measured here in Figure 1b ($[Br^-]_0 = 0.001$ M) at $\Delta\tau = 40$ min was $N_{EP} = 0.23$ and so $\nu = 3.85$. The smallest chain length was around zero in Figure 1a, $\Delta\tau = 5$ min. Actually, a calculated ν would be negative in this case, due to carboxyl radical losses, which were not taken into account in our simple chain length calculation. As this result shows, the above numbers are only rough estimates. This is because, well before the equivalence point, there is not enough bromine in the mixture to satisfy our assumption that the carboxyl radicals react mainly with bromine. Approaching the equivalence point, the yield of bromide ions decreases due to the reaction of carboxyl radicals with Ce^{4+}. Thus the actual chain length at the beginning of the experiment is always longer than the one estimated from N_{EP}. For example, numerical simulations suggest for the experiment shown in Figure 1a for $\Delta\tau = 20$ min an average chain length of $\nu = 0.82$, which is significantly higher than the estimated 0.59.

3.5. Effect of the Bromide Ion Concentration. As pointed out previously, there are two bromine containing radicals, which could participate in the chain reaction: (i) $^\bullet Br$, the free bromine atom in reaction R29 and (ii) $^\bullet Br_2^-$, the dibromine radical ion in reaction R40.

Thus the next step was to devise an experiment to answer the question, which radical plays a dominant role in our experiments? To this end we decreased the initial bromide concentration from 10^{-2} M in Figure 1a to 10^{-3} M in Figure 1b. The formation of the dibromine radical ion leads to an equilibrium:

$$^\bullet Br + Br^- \leftrightarrow {}^\bullet Br_2^-$$

In our experiments that equilibrium was shifted toward the dibromine formation, as the following calculation indicates. The relative amount of the free bromine atoms compared to the dibromine radical ion can be expressed from the above equilibrium (the equilibrium is a good approximation here because the forward and backward reaction rates are much faster, under the conditions applied in our experiment, than the rates of the reactions disturbing that equilibrium):

$$[^\bullet Br]/[^\bullet Br_2^-] = k_{-18}/(k_{18}[Br^-]) = (5.6 \times 10^{-6}\ \text{M})/[Br^-]$$

As the above formula shows, even in the case of the more dilute bromide ion solution ($[Br^-] = 10^{-3}$ M) 99.44% of the radicals are dibromine ion radicals, and only 0.56% are bromine atoms. In the more concentrated bromide solution the equilibrium is shifted even more toward the dibromine ion radical. If the reactions of the more abundant $^\bullet Br_2^-$ were dominating in the chain reaction over the reactions of $^\bullet Br$, then decreasing the bromide ion concentration would not affect the reaction rate considerably, because the fraction of dibromine radical ions is close to 100% in both solutions. If this were true, then the chain length would be about the same in 10^{-2} and 10^{-3} M bromide solutions. Comparing the "titration" curves in Figure 1a,b, however, shows that this is not the case: lowering the bromide concentration increases the kinetic chain length considerably. This result suggests that at least a great portion of the chain reaction proceeds via the very reactive bromine atoms. Naturally, this qualitative reasoning cannot exclude that dibromine radical ions do play some minor role in the chain reaction; only model calculations can give a more quantitative answer.

3.6. Modeling the Chain Reaction. First Step: Reducing the System. To make quantitative conclusions, we performed numerical simulations applying the rate constants of Table 1, using $k_G = k_{EV} = 2.5 \times 10^{-4}\ s^{-1}$ measured for the evaporation rate of bromine from the semibatch reactor and regarding the actual Ce^{4+} inflow. (See Appendix A for definition of k_G and k_{EV}.) The latter was taken into account as

$$\sigma(Ce^{4+}) = \phi(Ce^{4+})/V_R$$

where $\sigma(Ce^{4+})$ is the "physical" (i.e., not chemical) source density for Ce^{4+} in the reactor ($M \cdot s^{-1}$), $\phi(Ce^{4+})$ is the Ce^{4+} flux or inflow ($mol \cdot s^{-1}$), and V_R is the reactor volume (dm^3). As the reaction volume changed only 1% during the whole experiment, dilution effects due to the increased volume were neglected. Thus for $\sigma(Ce^{4+})$ the following formula was applied in the present calculations:

$$\sigma(Ce^{4+}) = 2 \times 10^{-3}\ M/\Delta\tau$$

where $\Delta\tau$ is the length of the experiment, the time required to increase the total cerium concentration ($[Ce^{3+}] + [Ce^{4+}]$) in the reactor from zero to 2×10^{-3} M. $\Delta\tau$ was 300, 600, 1200, or 2400 s, depending on the input flow rate. That physical source was added to the chemical kinetic terms in the balance equation for Ce^{4+}, to obtain this way the dynamic equation of that component in the semibatch experiment. For all other components batch conditions were assumed.

Naturally, not all reactions of Table 1 were "active" in the model calculations for the chain reaction. For example, no initial BrO_3^-, $HBrO_2$, Br_2O_4, or $BrO_2^\bullet$ was present in this case. As these "missing" components were not produced from other components of the chain reaction, reactions involving them were inactive here. Other reactions could be also neglected; e.g., the bromine hydrolysis was suppressed here, due to the presence of bromide ions in the chain reaction experiments. As a consequence of such simplifications, the reaction system could be reduced considerably. Numerical simulations proved that the subsystem of the following reactions: RG, R12, −R12, R18, −R18, R21, R26, R29, R33.1, R33.2, R34, and R40 together with the Ce^{4+} inflow were able to model the behavior of the whole system accurately in the case of chain reaction experiments. Process RG had only a minor effect on the simulation results as the evaporation loss of bromine was small here. Nevertheless, as k_{EV} was known from our "blank" measurements, RG was included in our model calculations. Rate constants for R2, R12, −R12, R18, −R18, R21, and R26 were known from the literature. The rate constant of R33.1 and R33.2 was assumed to be the same as that of an analogous reaction

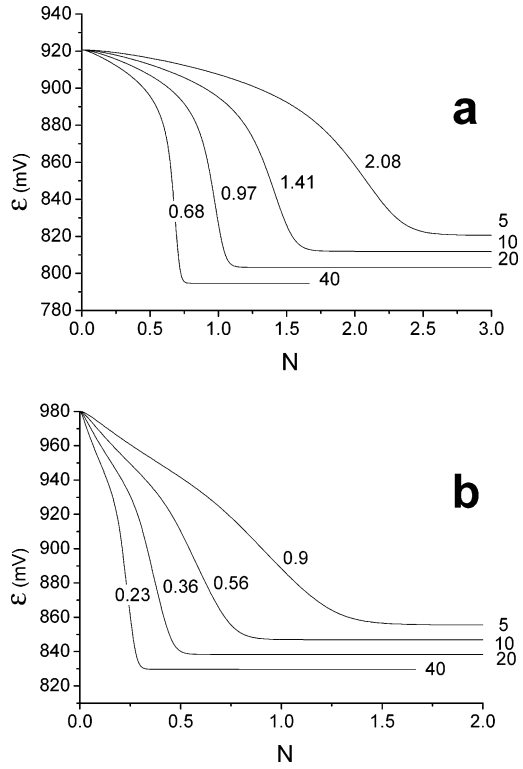

Figure 2. Calculated electrode potential−stoichiometric ratio *N* diagrams for the experiments shown in Figure 1a,b. The applied flow rates and the inflection points are indicated at each curve as in Figure 1.

between carboxyl radical anion and iodine measured by Schwarz and Bielski.[14]

Thus only three important reactions remained, namely, R29, R34, and R40, the rate constants of which had not been measured previously. As the actual choice of these rate constants affected the results of the simulations significantly, it seemed possible to estimate them by comparing experiments and simulations.

3.7. Numerical Simulations of the Chain Reaction. Estimated Rate Constants for the Bromine Atom−Oxalic Acid and for the Carboxyl Radical−Ce^{4+} Reactions. Simulated platinum electrode potential ϵ-stoichiometric ratio *N* diagrams are presented in Figure 2. The electrode potential was calculated from the actual bromine, bromide, and Ce^{4+} concentrations. (Method of the electrode potential calculation is given in Appendix B.)

The simulations shown in Figure 2 were performed with optimal values of rate constants k_{29} and k_{34} (optimal = reproducing best the experimental curves), whereas k_{40} was set to 0. Next we give these optimal values, some arguments supporting their choice, and some comments on the role of reactions R29, R34, and R40.

R29. The optimal value for k_{29} was found to be 7×10^5 M^{-1} s^{-1}. As R29, the reaction between bromine atom and oxalic acid is a part of the chain reaction, the kinetic chain length was determined mainly by this reaction, and simulation results were rather sensitive to this parameter. We found no previous experimental data in the literature. Earlier estimates[12,15] assumed that k_{29} is 2×10^3 M^{-1} s^{-1}. Though the present value is considerably higher, it is not unrealistic, as the few rate constants reported in the literature[8] for other bromine atom reactions are even higher.

R34. The optimum value for k_{34} was around 1.5×10^9 M^{-1} s^{-1} in our simulations. Thus R34, the reaction between carboxyl radical and Ce^{4+}, can be a rather fast reaction. Despite that, at lower flow rates, this chain termination step is not significant, except at the end of the chain reaction, when most of the initial bromine is consumed. (If there is enough bromine, then only R21, the self-recombination reaction of dibromine radical ions is the important chain termination reaction.) In the case of higher flow rates, however, R34 becomes more important. This is because at higher flow rates both the steady-state Ce^{4+} and the carboxyl radical concentration gets higher, and this way the relative weight of R34 increases. As a consequence of the more intense chain termination, the chain length becomes shorter and pushes N_{EP} to higher values. Thus, when k_{34} was chosen to be high enough in our simulations, the position and the shape of the titration curves became sensitive to the applied flow rate in accordance with the experiments. On the other hand, if smaller k_{34} were applied in the calculations, e.g., 10^6 or 10^7 M^{-1} s^{-1}, as suggested in earlier work,[12,15] then the simulated curves were too close to each other, and also steeper than the ones recorded in the experiments. We could not find any experimental value for k_{34} in the literature. Rate constants, however, reported for analogous reactions between the carbon dioxide radical anion and various Fe^{3+} complexes[8] can be as high as several times 10^9 M^{-1} s^{-1}. As Ce^{4+} is a stronger oxidant than Fe^{3+}, we think it is not unrealistic to assume that k_{34} is also in the same range.

R40. Model calculations for the chain reaction showed that its rate constant is certainly less than 100 M^{-1} s^{-1}. If that, or a higher value was applied, then the bromide concentration had less effect in the simulations than in the real experiments. Below 100 M^{-1} s^{-1}, however, the effect of this parameter was very small for the simulation results. Thus the reaction was neglected.

As can be seen, the experimental and the simulated titration curves (see Figures 1 and 2) agree rather well. At low flow rates, however, a slight deviation can be observed in the shape of the curves. The experimental curves reach their final potential values more slowly than the simulated ones. Because of this, the experimental curves look "smoother" than their simulated counterparts. The deviation is probably due to slowness of the bromine desorption from the Pt electrode. When, after the equivalence point, the bromine concentration drops to a low level in the bulk of the solution rapidly, then surface bromine, and consequently also the electrode potential, cannot follow that drop instantaneously, as desorption is slow at these low concentrations.

4. Modeling the Oscillatory System

4.1. Mechanism and Rate Constants. Simulations of the oscillatory BZ reaction of oxalic acid[1] were performed with the model given in Table 1.

In Table 1 we tried to collect all reactions that could play a role in the oscillatory system. Thus besides the inorganic subset of the BZ reaction (R1−R8), and the reactions of the chain reaction discussed in the previous paragraph, an attempt was made to regard all possible reactions of the four radical species—$^{\bullet}CO_2H$, $^{\bullet}Br$, $^{\bullet}BrO$, and $^{\bullet}BrO_2$—which can have a role here. For the actual values of the rate constants of Table 1 we applied four sources: (i) values reported already in the literature, (ii) k_0, k_{23}, k_{24}, $k_{25.1}$, and $k_{25.2}$ measured in the first part[1] of this work, (iii) k_{29}, k_{34}, and k_{40} determined here from chain reaction experiments, (iv) estimates based on rate constants of analogous reactions, and (v) k_{30} as the only parameter, which was not fixed but was varied to achieve an acceptable consonance between the simulations and the experiments. Another rate constant, k_{42} was also varied a little, but its effect regarding the overall dynamics is minor compared to that of k_{30}.

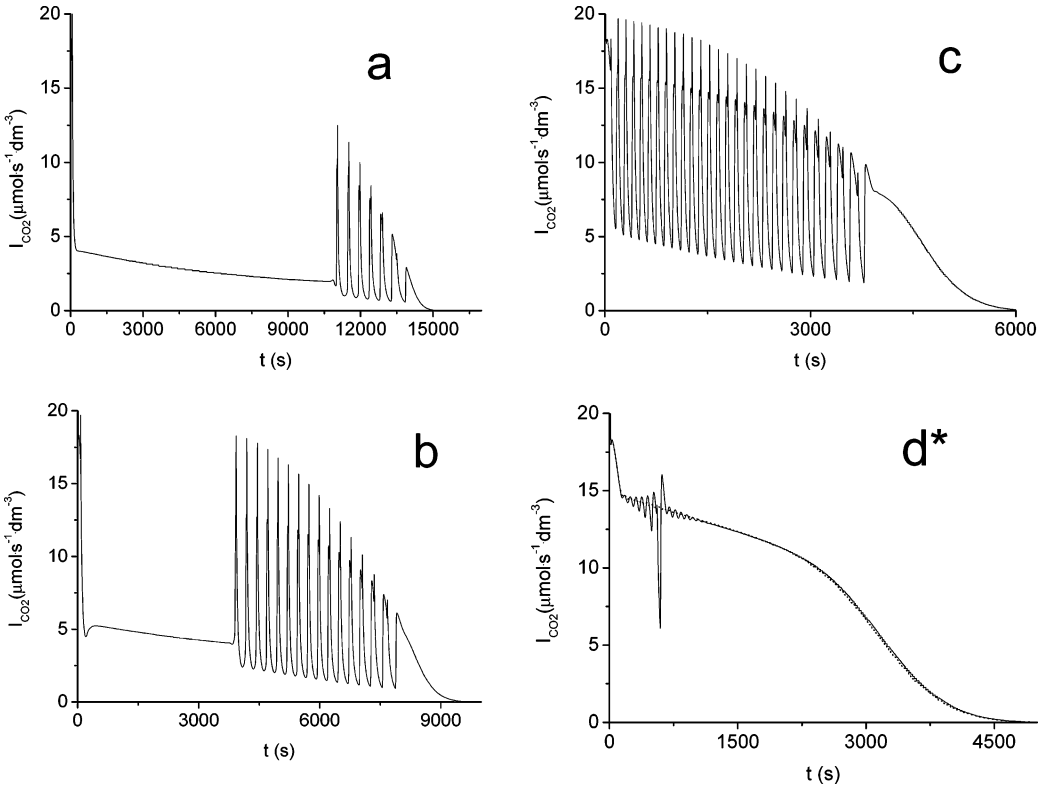

Figure 3. Simulated dynamics of the BZ reaction with oxalic acid as a function of the bromine removal rate k_G. Initial concentrations: $[NaBrO_3]_0 = 21$ mM, $[OA]_0 = 20$ mM, $[Ce(SO_4)_2] = 0.5$ mM, $[H_2SO_4] = 1$ M. $T = 20$ °C. k_G values: (a) 3.1×10^{-3} s^{-1}, (b) 5.7×10^{-3} s^{-1}, (c) 11.4×10^{-3} s^{-1}, (d*) 18.0×10^{-3} s^{-1} (continuous line), and 18.2×10^{-3} s^{-1} (dotted line). For (a), (b), and (c) all parameters are the same as for the experimental curves in Figure 1a−c in our first paper on this reaction.[1]

The next paragraph discusses briefly grounds for the estimations applied in (iv) and (v).

4.2. Basis of the Rate Constant Estimations.

R9. Order of magnitude estimation based on the assumption that k_9 is between k_8 and k_{10}.

R10. Zhang and Field[16] suggested the same rate constant for the analogous reaction of Mn^{2+} with the bromine atom.

R13. Rate constants for the self-recombination reaction of $^{\bullet}BrO$ and also of $^{\bullet}BrO_2$ radicals is 3×10^9 according to NHR.[8] Our estimate is based on these analogies.

R14, R16. In cases when no experimental data were available for the rate constant of a self-recombination or a cross-recombination reaction of bromine or oxybromine radicals, the value of 3×10^9 M^{-1} s^{-1} was applied.

R17. For an analogous reaction between the dibromine radical ion and the bromite ion Buxton and Dainton[23] found a rate constant of 8×10^7 M^{-1} s^{-1}. As a free bromine atom is more reactive, we assumed about an order of magnitude higher value for k_{17}.

R20. Basis of the estimation: the rate constant of the analogous reaction between the dichlorine radical ion and Ce^{3+} is 1×10^4 M^{-1} s^{-1} according to NHR.[8] We assumed that a similar reaction with dibromine radical ion is slower.

R28. It was found by Field and Boyd,[12] and also by us,[1] that the analogous reaction R27 between oxalic acid and the $BrO_2^{\bullet}$ radical is rather slow. Thus we assumed that k_{28} is similarly slow.

R30. The rate constant value for the analogous reaction between the carbon dioxide radical anion and the iodate ion is 1.3×10^8 M^{-1} s^{-1} according to Buxton and Sellers.[24] As the dynamics of the reaction was rather sensitive to this parameter, its value was fitted to obtain realistic results in the model calculations. In our calculations the optimal value for this rate constant was 1.0×10^7 M^{-2} s^{-1}.

R31. It was assumed that k_{31} is between k_{30} and k_{32}: order of magnitude estimate.

R32. An analogous reaction between the carbon dioxide radical anion and hypoiodous acid is known. Its rate constant reported by NHR[8] was accepted as an estimate for k_{32}.

R36. It was assumed that R36 is somewhat faster than R33 or R35.

R37, R38. It was assumed that $k_{37} = k_{38} = k_{33}$.

R42, R43, and R44. These are all recombination reactions of bromine containing free radicals. As in the case of R14 and R16, a rate constant of 3×10^9 M^{-1} s^{-1} was applied. R42 was an exception, however; its value was chosen as 1×10^9 M^{-1} s^{-1}. This is because k_{42}, unlike the other radical−radical recombination reactions, influenced the dynamics, and a smaller value gave somewhat better agreement between experiments and simulations.

4.3. Comparison of the Simulations with the Experiments. The simulations were performed by applying the same initial concentrations and bromine removal rates as in the experiments.[1] The results (calculated CO_2 evolution rates as a function of time for various k_G parameter values) are shown in Figure 3.

The fine details of the CO_2 evolution rate curves cannot be recorded experimentally, because the measuring system transforms these sharp curves to smoother CO_2 current vs time diagrams, when the CO_2 is transported from the reactor to the detector by the nitrogen carrier gas. The time constant of the system is determined mainly by the CO_2 transfer from the liquid to the gas phase. Model calculations (not shown here) performed in the time constant range of our system (10−30 s) indicate that such a smoothing practically eliminates the very sharp needles (appearing on the top of nearly all wide peaks), but the

wider peaks themselves are unaffected or affected only slightly. Thus, when comparing simulated diagrams with the experimental ones, calculated peak heights will be regarded without the sharp needles, which cannot be observed experimentally.

Confronting now the results of the simulations with that of the experiments in Figure 3a,b, the agreement is satisfactory on a qualitative level: oscillations appear only after a long induction period in both cases, and in Figure 3b the induction period is shorter than in Figure 3a. Nevertheless, the simulated induction periods and also the oscillatory regimes are about 20% longer than the experimental ones, and simulations produce somewhat more oscillations than experiments. Moreover, the peak heights in the simulations (without the sharp needles) are 20−40% smaller than in the experiments. All these indicate that the overall reaction is faster in the real system than in the simulations.

The agreement is less satisfactory in the case of Figure 3c, where the oscillatory region and also the number of oscillations is roughly doubled and the amplitude is halved, compared to the experiments. In the model the oscillations disappear at a lower k_G value than in the experiments. In the simulations at $k_G = 18.0\ s^{-1}$ mostly small amplitude oscillations can be observed which cease, however, at $k_G = 18.2\ s^{-1}$ (these curves are shown in Figure 3d*). In the experimental system the large amplitude oscillations continue to exist until $k_G = 20.8\ s^{-1}$ where they also disappear in a supercritical Hopf-like bifurcation. Nevertheless, even above $k_G = 20.8\ s^{-1}$, where both experiments and model calculations display a nonoscillatory behavior, the rate of the CO_2 evolution is about 2 times higher in the experiments than in the simulations, and as a consequence the reaction time is about twice as long in the simulations. This indicates again that simulations underestimate the overall rate of the reaction.

4.4. Reactions Important in the Modeling of the Oscillatory System. Among the 45 reactions (RG + R1−R44) of Table 1, there are only 22 that contribute significantly to the modeling of the oscillatory system. These are the following reactions: RG, R1−3, R6−9, R14−15, R18, R22−23, R25.1, R25.2, R26, R29−30, R33.1, R34, R41, and R42. Simulations repeated with the subset of these important reactions in the relevant parameter range of k_G gave results very close to the ones obtained by applying the full system of Table 1. It is interesting to remark that R15, the production of the $^{\bullet}BrO$ radical, its disproportionation (R22), and its reaction with bromous acid (R41) and with $^{\bullet}BrO_2$ (R42) are among the important reactions.

5. Conclusions and Outlook

This research was started in the hope that to elucidate the mechanism of the BZ reaction with its simplest organic substrate would be a relatively easy task. Although this is certainly true compared to other BZ systems, we had to realize that, even in this simple case, it is not so easy to reveal all the reactions playing an important role in the oscillations. Actually, we believe that some important reactions are still missing from our scheme, and it would be important to find these reactions. It is a major obstacle in unfolding of complex reaction mechanisms, however, that in most cases the individual reactions cannot be studied independently of each other. This is especially true for radical reactions.

Whereas the isolated study of a specific reaction is usually not feasible, it is possible to find subsystems where not all the reactants of the full BZ system, but only a part of them plays a role. Thus our strategy was to create and study such subsystems where rate constants of important individual reactions could be determined. Pursuing that strategy, in the first part of our work[1] we measured the bromine removal rate k_G as a function of the carrier gas flow and studied reactions of oxalic acid with acidic bromate, bromous, and hypobromous acids. These were oxygen atom transfer reactions from the above-mentioned oxybromine species to the oxalic acid substrate. No radical intermediates were detected in these processes. In the presence of Ce^{4+}, however, various radicals, $^{\bullet}CO_2H$, $^{\bullet}BrO_2$, $^{\bullet}BrO$, $^{\bullet}Br$, and $^{\bullet}Br_2^-$, and their reactions appear, causing a fundamental change in the mechanism.

Thus one aim in this second part was to collect data about the radical reactions. To this end we created and studied a new subsystem, the oxalic acid−bromine chain reaction, mediated by a Ce^{4+} inflow. From the above-mentioned five radicals, only three (carboxyl radical, bromine atom, and dibromine radical ion) play a role in the chain reaction. In this subsystem rate constants of the oxalic acid−bromine atom and the Ce^{4+}−carboxyl radical reactions were determined. It was also found that $^{\bullet}CO_2H$ radicals react very rapidly with elementary bromine. This explains the somewhat surprising result that the reduction of bromine is achieved by the inflow of an oxidant, namely Ce^{4+}, into the reactor. (It is interesting to mention that elementary bromine appears in various BZ oscillators[25,26] as well, thus the carboxyl radical−bromine reaction might have a more general importance.)

Simulation of the chain reaction indicated that the rate of the oxalic acid−$^{\bullet}Br_2^-$ radical ion reaction is more than 3 orders of magnitude slower than the oxalic acid−$^{\bullet}Br$ atom reaction; thus the former can be neglected under the conditions applied here.

On the basis of our new results, we simulated the oscillatory BZ reaction of oxalic acid. For this purpose the newly determined rate constants were combined with a recent set of rate constants known from previous research on the BZ reaction.[2] Further rate constants were collected from the literature or were estimated on the basis of analogies. In the simulations we applied these rate constants without any further modifications, and only one of them, k_{30}, was used as a variable parameter to fit the experiments.

We found a satisfactory agreement between the simulations and the experiments only at low carrier gas flow rates (at low k_G values). Even at these low flow rates, however, the calculated reaction rates were smaller than the experimental ones. At higher k_G values the deviation became more pronounced.

The reason for the disagreement between simulations and experiments is not clear presently. Naturally, one possibility is that the deviation is due to inaccuracy in the estimated rate constants. Though such errors certainly exist, we think it is more probable that the deviations are caused by one or more unknown reactions, which play an important role in the oscillatory system. In the classical BZ reaction unknown reactions can be found usually in the organic subset. This cannot be the case here, because care was taken to include all possible reactions of the two organic components into Table 1 (reactions of oxalic acid (R23−R29) and of carboxyl radical (R30−R39)). Thus, if there are any unknown reactions, they should be in the inorganic subset. Research is in progress to investigate this possibility.

Finally, we should like to make two additional comments. (i) Our results prove that the Ce^{4+}−oxalic acid reaction can be applied as an effective carboxyl radical source, and reductions by that radical can be achieved in a semibatch reactor even in the presence of the oxidative Ce^{4+} (whose steady-state concentration in such a reactor is low, however). (ii) It seems that the $^{\bullet}BrO$ radical plays a role in the BZ reaction. That idea was

suggested originally by Rovinsky and Zhabotinsky[27] in 1978 but was not applied since then.

Acknowledgment. We thank Maria Liria Turco Liveri, Renato Lombardo, Attila Horváth, and Henrik Farkas for helpful discussions. This work was partially supported by OTKA T-042708 and M-045272 grants and the ESF Program: "Reactor".

Appendix A

In the case of the first "blank" experiment the bromine removal is a physical process associated with no chemical reaction. The measured voltage ϵ in that experiment can be written as

$$\epsilon = \varphi_0 + 25.2\ \text{mV} \ln \frac{\sqrt{[\text{Br}_2]}}{[\text{Br}^-]_0}$$

where φ_0 is a constant voltage and $[\text{Br}^-]_0$ is the constant bromide concentration. The time derivative of ϵ is

$$\frac{\text{d}\epsilon}{\text{d}t} = 12.6\ \text{mV} \frac{1}{[\text{Br}_2]} \cdot \frac{\text{d}[\text{Br}_2]}{\text{d}t}$$

As the physical removal rate of bromine is proportional with its concentration

$$\frac{\text{d}[\text{Br}_2]}{\text{d}t} = -k_{\text{EV}}[\text{Br}_2]$$

k_{EV} can be calculated as

$$k_{\text{EV}} = (-\text{d}\epsilon/\text{d}t)/12.6\ \text{mV}$$

Presently, the physical process removing bromine is evaporation; thus k_{EV} is a "rate constant" of evaporation. Naturally, this rate depends on the geometry of the reactor and the stirring rate, but these parameters were held constant in the chain reaction measurements. The bromine loss was minimal in these experiments, because there was no gas bubbling. If a gas flow is applied, however, like in the experiments of the first part,[1] the bromine removal rate can be much higher. In that paper the "rate constant" was denoted by k_{G}. Obviously, both k_{EV} and k_{G} denote the rate constant of the same process: the physical removal of bromine. The different notation was applied only to emphasize that though k_{EV} is small and held constant, k_{G} is much larger and it is used as a bifurcation parameter. (It is interesting to remark, as one of our referees pointed out, that in principle a variable magnetic stirring rate could be also applied as a bifurcation parameter.)

Appendix B

When both bromine and bromide are present, the potential of the Pt electrode is determined mainly by the bromine−bromide redox couple. Nevertheless, when the bromine concentration is low, a contribution due to Ce^{4+} can be also observed, which can be described by a Nicolsky−Eisenman[28] type expression, where the Ce^{4+} concentration (multiplied by a selectivity coefficient) is added to the bromine concentration in the electrode potential formula. Thus the measured voltage ϵ at 20 °C can be given as

$$\epsilon = \epsilon_0 + 25.2\ \text{mV} \ln \frac{\sqrt{[\text{Br}_2] + 0.002[\text{Ce}^{4+}]}}{[\text{Br}^-]_0}$$

where ϵ_0 was 893 mV in our experiments and $[Ce^{4+}]$ is the steady-state Ce^{4+} concentration in the semibatch reactor. The selectivity factor 0.002 was determined experimentally. A possible explanation for the above formula is the following. Most probably, the Pt electrode responds always to the bromine. However, when the bromine concentration in the bulk falls to a very low value, then some minute amount of bromine on the surface can become significant. If we assume that the platinum surface catalyzes the oxidation of bromide by Ce^{4+} to bromine then this surface bromine can be a potential determining factor. That potential determining surface concentration of bromine should be proportional with the rate of the surface reaction which is, in turn, proportional with the Ce^{4+} concentration of the solution. It is the sum of the surface and the bulk bromine that determines the potential. The second term, however, can be observed at very low bromine concentrations only.

References and Notes

(1) Pelle, K.; Wittmann, M.; Lovrics, K.; Noszticzius, Z.; Turco Liveri, M. L.; Lombardo, R. *J. Phys. Chem. A* **2004**, *108*, 5377.
(2) Hegedüs, L.; Wittmann, M.; Noszticzius, Z.; Yan, S.; Sirimungkala, A.; Försterling, H. D.; Field, R. J. *Faraday Discuss.* **2001**, *120*, 21.
(3) Zhabotinsky, A. M. *Biofizika* **1964**, *9*, 306.
(4) *Oscillations and Traveling Waves in Chemical Systems*; Field, R. J., Burger, M., Eds.; Wiley: New York, 1985.
(5) In 3 M sulfuric acid, applying appropriate conditions, oscillations were observed even without any physical bromine removal: Ševčik, P.; Adamčiková, L. *J. Chem. Phys.* **1989**, *91*, 1012.
(6) Epstein, I. R.; Pojman, J. A. *An Introduction to Nonlinear Chemical Dynamics*; Oxford University Press: New York, 1998.
(7) Sirimungkala, A.; Försterling, H. D. Unexpected Kinetics in the Ce(IV)−Oxalic Acid Reaction. MS submitted to *J. Phys. Chem. A.*
(8) Neta, P.; Huie, R. E.; Ross, A. B. *J. Phys. Chem. Ref. Data* **1988**, *17*, 1027.
(9) Buxton, G. V.; Sellers, R. M. *J. Chem. Soc., Faraday Trans. 1* **1973**, *69*, 555.
(10) Smith, R. J. *Aust. J. Chem.* **1972**, *25*, 2503.
(11) In theory the rate constant of the molecular HOBr−oxalic acid reaction could be determined from such measurements. To this end, however, a different reactor (a tightly sealed one) would be necessary, as the uncertainty caused by the bromine evaporation in the present experiments prevented us to make a reliable estimate of that rate constant.
(12) Field, R. J.; Boyd, P. M. *J. Phys. Chem.* **1985**, *89*, 3707.
(13) Hlaváčová, J.; Ševčik, P. *Chem. Phys. Lett.* **1991**, *182*, 588.
(14) Schwarz, H. A.; Bielski, B. H. J. *J. Phys. Chem.* **1986**, *90*, 1908.
(15) Györgyi, L.; Turányi, T.; Field, R. J. *J. Phys. Chem.* **1990**, *94*, 7162.
(16) Field, R. J.; Zhang, Y. X. *J. Phys. Chem.* **1990**, *94*, 7154.
(17) Nagarajan, V.; Fessenden, R. V. *J. Phys. Chem.* **1985**, *89*, 2330.
(18) Wong, D.; DiBartolo B. *J. Photochem.* **1975**, *4*, 249.
(19) Morliere, P.; Patterson, L. K. *Inorg. Chim. Acta* **1982**, *64*, L183.
(20) Kläning, U. K.; Wolff, T. *Ber. Bunsen-Ges. Phys. Chem.* **1985**, *89*, 243.
(21) Flyunt, R.; Schuchmann, M. N.; von Sonntag, C. *Chem. Eur. J.* **2001**, *7*, 796.
(22) Amichai, O.; Treinin, A. *J. Phys. Chem.* **1970**, *74*, 3670.
(23) Buxton, G. V.; Dainton, F. S. *Proc. R. Soc. (London) Ser. A* **1968**, *304*, 427.
(24) Buxton, G. V.; Sellers, R. M. *J. Chem. Soc., Faraday Trans. 1* **1985**, *81*, 449.
(25) Kumli, P. I.; Burger, M.; Hauser, M. J. B.; Müller, S. C.; Nagy-Ungvárai, Zs. *Phys. Chem. Chem. Phys.* **2003**, *5*, 5454.
(26) Rastogi, R. P.; Husain, M. M.; Chand, P.; Misra, G. P.; Das, M. *Chem. Phys. Lett.* **2002**, *353*, 40.
(27) Rovinskii, A. B.; Zhabotinskii, A. M. *Teor. Eksperim. Khim.* **1978**, *14*, 183.
(28) Umezawa, Y.; Bühlmann, P.; Umezawa, K.; Tohda, K.; Amemiya, S. *Pure Appl. Chem.* **2000**, *72*, 1851.